Theoretical Study on Silver- and Gold-Loaded Zeolite Catalysts: Thermodynamics and IR Spectroscopy

Anibal Sierraalta,*,† Rafael Hernandez-Andara,† and Elena Ehrmann‡

Laboratorio de Química Computacional, Centro de Química, Instituto Venezolano de Investigaciones Científicas, Apartado 21827, Caracas 1020-A, Venezuela, and Departamento de Química, Universidad Simón Bolívar, Apartado 89000, Valle de Sartenejas, Baruta-Edo Miranda, Venezuela

Received: June 22, 2006; In Final Form: July 20, 2006

Density functional calculations have been carried out to determine geometries, adsorption energies and vibrational frequencies of NO, N_2O, CO, O_2, and H_2O, on a model for Ag(I) and Au(I) ion-exchanged ZSM-5 catalysts. Using statistical mechanics, the ΔH and ΔG values were calculated in order to evaluate the stability of the adsorbates on Ag(I) and Au(I) sites. The calculated vibrational frequencies are in reasonable agreement with the reported experimental values. The analysis of the results shows that at 475 °C the adsorption of two NO molecules and the direct N_2O decomposition on AgZSM-5 are thermodynamically unfavorable. The adsorption of one NO molecule presents a small positive ΔG value. On the contrary, in the case of AuZSM-5, the adsorption of one NO molecule and the direct N_2O decomposition to produce N_2 are thermodynamically favorable. For both models, the N_2O decomposition by AgO and AuO species is thermodynamically very favorable. The analysis of the interaction with H_2O shows that water displaces the adsorbed NO on AgZSM-5 but not on AuZSM-5 which indicates that the AuZSM-5 catalyst is less sensitive to deactivation by H_2O than the AgZSM-5 catalyst.

Introduction

One of the main targets in environmental catalysis is the elimination of nitrogen oxides emissions by mobile and stationary sources because these nitrogen oxides (NO_x) are among the most air quality damaging pollutants. Despite the large thermodynamic driving force, the reduction of nitrogen oxides at temperatures below 800 °C is extremely slow in the absence of a catalyst.[1] Currently, the commercial catalytic process for NO_x emission control in stationary sources is performed with ammonia and titania-supported vanadia.[2−5] The main drawbacks of this process are the corrosive and toxic effects of ammonia. A suitable catalyst could overcome those problems associated with the use of ammonia. There has been a tremendous amount of catalysts developed for the catalytic reduction of the NO_x, among them, the transition metal exchanged catalysts from which the CuZMS-5 has been the most extensively studied one due to its good catalytic performance. Unfortunately, water, O_2 and SO_2 deactivate this catalyst.[1,6−8] In the search of a better catalyst, other systems such as Fe−ZMS-5,[9−14] Co−ZMS-5,[15−19] Au−MFI,[20−24] Ag−MFI,[25−30] etc. have been studied.

Different structures for the active site have been proposed in the literature to explain the catalytic activity of AgZSM-5 in the selective catalytic reduction (SCR) of NO_x. Satsuma[31] and Shimizu[32] proposed that the active site corresponds to a cationic silver cluster, Ag_n^+. Aika et al.[26,27] using H_2−TPR, N_2O−TPD, and XRD, concluded that the silver is present mainly as exchanged Ag ions and in the form of a certain type of Ag_2O clusters. Bao and colleagues[29] found that during the SCR of NO_x by CH_4 and excess of O_2, the reaction induces a Ag restructuring that results in the formation of *ill-defined* silver oxides. They concluded that the isolated silver ions are the key species in the SCR of NO_x.[25] Anpo et al.[30,33−36] using different spectroscopic techniques, concluded that isolated Ag^+ ions are the main silver species within the AgZSM-5 catalyst and therefore the most probable active sites. Li and Flytzani-Stephnopoulos[28] studied the promotion of AgZSM-5 by cerium and found that a minor amount of Ag exists as dispersed Ag^+ ions, while the major Ag fraction appears as silver nanoparticles. From their study, they concluded that the dispersed Ag^+ ions are active sites for $DeNO_x$ while the nanoparticles catalyze the methane combustion reaction.

In spite that AgZSM-5 and AuZSM-5 have shown good SCR performance, they still do not meet the requirements for commercial applications. To improve these systems, it is essential to understand the role of silver and gold in Ag/Au−ZSM5, in the selective reduction of NO_x to N_2. To shed some light on this problem, we have undertaken quantum chemical modeling to determine the IR frequencies and the thermodynamic properties of H_2O, O_2, NO, and N_2O molecules adsorbed on AgZSM-5 and AuZSM-5 models. In this work we analyze, from the quantum chemistry point of view, the physical-chemical properties and reactivity of the Ag(I) and Au(I) ions supported on a zeolite type site. Even though, different oxidation or aggregation states can be present in the real catalyst,[21,24,28−29,31−32] there is a common consensus in the literature that Ag(I) and Au(I) are the catalytically active species.

Computational Details and Models

All geometry optimizations, energy and frequency calculations were performed using Gaussian-98 program,[37] at B3LYP level with the 6-31G(d) basis set for H, Si and Al atoms. The relativistic Stevens effective core potential (CEP-121) with its corresponding basis set was employed for Ag and Au; and the

* Corresponding author. E-mail: asierral@ivic.ve.
† Laboratorio de Química Computacional, Centro de Química, Instituto Venezolano de Investigaciones Científicas.
‡ Departamento de Química, Universidad Simón Bolívar.

10.1021/jp063911p CCC: $33.50
Published on Web 08/23/2006

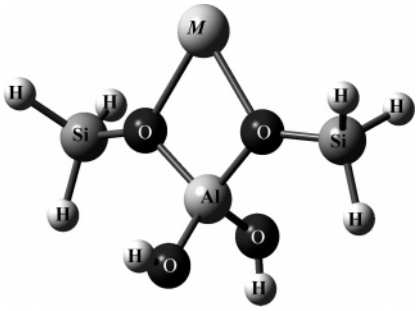

Figure 1. M-T3 model employed in the calculations, showing the position of the metallic ion. M = Ag^+, Au^+.

full-electron 6-311G(d,p) basis set was used for C, N, and O atoms. Frequency calculations were performed using the minimum energy structures. No scaling factor was applied to the calculated vibrational frequencies. The charge analysis was performed using the natural bonding analysis, NBO method.

The active site of the AgZSM-5 and AuZSM-5 catalysts was modeled by an Ag-T3 and Au-T3 site. The T3 site, $[H_3SiOAl(OH)_2OSiH_2]^-$, is composed by three tetrahedrons (T3) and model a Brønsted site of one zeolite. The metallic ion, Ag^+ or Au^+, was set on bridge between two oxygen atoms (see Figure 1,) according to the experimental results of Anpo et al.[30,33,34] We,[38−40] as well as other authors[33,41−43] used similar models to model a possible exchange site inside a zeolite framework. In the models employed in this work, physical-chemical effects such as electrostatics or van der Waals type interactions present in the zeolite framework were not considered. However, it is expected that these effects have no qualitative effect upon the results since the size of the adsorbed molecules is small compared to the zeolite pores or rings.

Results and Discussions

Silver(I) Zeolite. According to Anpo's experimental results,[30,33,34] silver atoms in the AgZSM-5 catalyst prepared by ion-exchange methods, are present as isolated bicoordinated Ag^+ ions. To model this system, one Ag^+ ion was set on a bridge between two oxygen atoms as shown in Figure 1. To test this model, vibrational frequencies for several selected free molecules and for NO and CO adsorbed on Ag, were calculated and compared with experimental values (see Table 1.) According to the results, the methodology and basis set employed in this work led to a 1 to 6% overestimation of the vibrational frequencies. The differences between the calculated and the experimental frequencies for the adsorbed NO, CO, and N_2O molecules on the ZAg catalyst vary from 1 to 7%. These values lie within the uncertainty of the method (1 to 6%), which indicates that the selected model reproduces, with a certain degree of confidence, the active site of the AgZSM-5 catalyst. The calculated values for the N_2O vibrational stretching frequencies, υ_{NN} 2404 and υ_{NO} 1368 cm^{-1}, are in reasonable agreement with the previously reported theoretical values of 2269 and 1322 cm^{-1} [33] for a similar model, considering that the former values are scaled.

Table 2 shows some geometrical properties and net charges for the ZAg model studied here. As expected, the Ag net charge is close to +1 (+0.88e) since Ag occupied the Brønsted acid site. In general, the net charge on the Ag atom does not change after NO, N_2O, CO, O_2, or H_2O adsorption, indicating that no important charge transfer takes place. The similarity of the vibrational frequencies between the adsorbed and the corresponding free molecules confirms this result. For example, the υ_{CO} in ZAgCO (υ_{CO} = 2217 cm^{-1}), is very close to the υ_{CO} of the free molecule (υ_{CO} = 2219.8 cm^{-1}.) The NBO analysis shows that the NO molecule in ZAgNO, ZAgON, $ZAg(NO)_2$ η^1-N, and $ZAg(NO)_2$ η^1-O is neutral. This agrees with the N−O and R(N−O) distance values as well as the υ_{NO} values, which are closer to those of to the free NO molecule than those of the AgNO species (R(N−O) = 1.16 Å, υ_{NO} = 1768.9 cm^{-1}, q_{NO} = −0.15 e) and $AgNO^+$ (R(N−O) = 1.13 Å, υ_{NO} = 2008.6 cm^{-1}, q_{NO} = +0.13 e).

TABLE 1: Experimental and Theoretical Frequencies (υ) of AgNO, $AgNO^+$, AgCO, $AuCO^+$, and $AuNO^+$ Free Molecules and NO, CO, and N_2O Free and Adsorbed on AgZSM-5 Catalyst

		wavenumber (cm^{-1})		
assignment		experimental	this work	$\Delta\epsilon$ (%)[i]
AgNO+		1910.9[a]	2008.6	+5.1
AgNO		1711.8, 1707.3[a]	1768.9	+3.3, +3.6
AgCO+		2233.1[b]	2317.7	+3.8
AuCO+		2236.8[b]	2306.8	+3.1
AuNO+		1921.2, 1917.8[c]	2014.0	+4.8, +5.0
NO		1904.2[d]	1988.4	+4.4
CO		2169.8[d]	2219.8	+2.3
O_2		1580.2[d]	1641.9	+3.9
H_2O		3756.0[d]	3853.1	+3.0
N_2O	υ_{NN}	2224.0[d]	2355.8	+5.9
	υ_{NO}	1285.0[d]	1336.6	+4.0
ZAg(I)-NO		1908[e]	1927	+1.0
$ZAg(I)-(NO)_2$		1744[e]	1807	+3.6
ZAg(I)-CO		2192, 2190[e,f,h]	2217	+1.1, +1.2
$ZAg(I)-N_2O$	υ_{NN}	2256, 2251[f,g,h]	2404	+6.6, +6.8
	υ_{NO}	1325[f]	1368	+3.2

[a] Reference 55. [b] Reference 56. [c] Reference 57. [d] Reference 58. [e] Reference 45. [f] Reference 35. [g] Reference 30. [h] ref 33. [i] $\Delta\epsilon$(%) percentage difference between the theoretical and the experimental value.

Frequency calculations show that for NO adsorbed η^1-N and η^1-O, the υ_{NO} values are almost equal. Thus, it seems unfeasible to determine the NO adsorption mode using only experimental IR frequencies. To get insight into which adsorption mode is more stable under the experimental reaction conditions, ΔH and ΔG calculations were performed at 748 K (475 °C). This temperature was chosen because generally, the $DeNO_x$ reaction reaches a maximum NO conversion between 350 and 550°C. To test the accuracy of the results, calculations of ΔH and ΔG for the transformation of two NO molecules into N_2 and O_2, and the CO adsorption on our ZAg model were performed and compared with the experimental values. According to the calculation, the difference between the calculated and experimental values for the transformation of the NO (see reaction 19 in Table 3) is close to 1.0 kcal/mol. For the CO adsorption at 303 K, the calculate ΔH value is 2.2 kcal/mol below the experimental value.[44] Thus, the error in the values of ΔH and ΔG at 748 K can be estimated at around 2 kcal/mol.

Table 3 shows that $\Delta G > 0$ for the NO adsorption (reactions 1 and 4) on the ZAg catalyst. The η^1-N adsorption mode (reaction 1) is more exothermic; that is, thermodynamically more favored (lower ΔG) than the η^1−O mode (reaction 4). Consequently, the preferential NO adsorption mode should be η^1-N. Calculations for the adsorption process of two NO molecules yield a large positive ΔG value, which indicates that this is an unfavorable process. Thus, under standard reaction conditions (low NO concentration, high temperature,) $ZAg(NO)_2$ concentration will be negligible. This agrees with the experimental observations according to which a pressure increase above 61 Torr at 296 K is necessary in order to observe $ZAg(NO)_2$ formation.[45] The formation of the $ZAg(NO)_2$ and $ZAg(ON)_2$ complexes (reactions 2, 3, and 5) are spin-forbidden; i.e., they include spin changes. These kinds of reactions proceed through

TABLE 2: Geometries, Atomic Charges, Vibrational Frequencies and Spin Multiplicity (*S*) for the AgZSM-5 Model (ZAg)[a]

molecular system	geometrical properties			Ag charge	adsorbate net charge	freq (cm^{-1})
ZAg	*R*(Ag−Oa)	*R*(Ag−Al) = 3.05 Å				
S = 1	2.27 Å	α(Oa-Ag−Ob) = 53.3°		+0.88		
ZAgNO	*R*(Ag−N)	*R*(N−O)	α(Ag−N−O)			υ_{NO}
η^1-N, *S* = 2	2.13 Å	1.15 Å	134.0°	+0.89	−0.05	1927
ZAgON	*R*(Ag−O)	*R*(N−O)	α(Ag−O−N)	+0.86	+0.02	υ_{NO}
η^1-O, *S* = 2	2.41Å	1.15 Å	132.9°			1926
$ZAg(NO)_2$	*R*(Ag−N)	*R*(N−O)	α(Ag−N−O)	+0.91	−0.04	υ_{NO}
η^1-N, *S* = 1	2.23 Å	1.15 Å	118.9°			1918
$ZAg(NO)_2$	*R*(Ag−O)	*R*(N−O)	α(Ag−O−N)	+0.82	0.00	υ_{NO}
η^1-O, *S* = 1	2.49 Å	1.14 Å	135.8°			1950
	R(Ag−O)	*R*(O−N)				υ_{NO}
ZAg(ONNO)	2.35 Å	1.24 Å	α(Ag−O−N)	+0.86	+0.03	1466
η^1-O, *S* = 1		*R*(N−N)	123.3°			
		1.17 Å *R*(NN−O)				
		1.19 Å				
ZAgCO	*R*(Ag−C)	*R*(C−O)	α(Ag−C−O)	+0.84	+0.01	υ_{CO}
η^1-C, *S* = 1	2.04Å	1.13 Å	179.8°			2217
$ZAgOH_2$	*R*(Ag−O)	*R*(O−H)	α(Al−Ag−O)	+0.84	+0.05	υ_{OH}
η^1-O, *S* = 1	2.28Å	0.97 Å	176.9°			3757
$ZAgO_2$	*R*(Ag−O)	*R*(O−O)	α(Ag−O−O)	+0.88	−0.01	υ_{OO}
η^1-O *S* = 3	2.15Å	1.23 Å	125.3°			1587
$ZAgN_2O$	*R*(Ag−N)	*R*(N−N)	α(Ag−N−N)	+0.87	+0.00	υ_{NN}
η^1-N, *S* = 1	2.23Å	1.13 Å	177.9°			2404
		R(N−O)				υ_{NO}
		1.17 Å				1368
$ZAgON_2$	*R*(Ag−O)	*R*(N−N)	α(Ag−O−N)	+0.86	+0.02	υ_{NN}
η^1-O, *S* = 1	2.43Å	1.12 Å	132.0°			2365
		R(N−O)				υ_{NO}
		1.19 Å				1304

[a] Free molecule: N−O (NO) 1.15 Å, C−O (CO) 1.13 Å, O−H (H_2O) 0.97 Å, N−O (N_2O) 1.18 Å, N−N (N_2O) 1.13 Å, and O−O (O_2) 1.21 Å.

TABLE 3: Calculated Δ*H* and Δ*G* of Reaction at 748 K (in kcal/mol) for the AgZSM-5 Model (ZAg)

eq no.	reaction (adsorption)	Δ*H*	Δ*G*
1	ZAg + NO ⇄ ZAgNO (η^1-N)	−12.5	+6.8
2	ZAgNO (η^1-N)+ NO ⇄ $ZAg(NO)_2$ (η^1-N)	+11.4	+34.8
3	ZAg + 2NO ⇄ $ZAg(NO)_2$ (η^1-N)	−1.1	+41.6
4	ZAg + NO ⇄ ZAgON (η^1-O)	−3.9	+11.1
5	ZAgON (η^1-O)+ NO ⇄ $ZAg(ON)_2$ (η^1-O)	+31.5	+52.6
6	ZAg + CO ⇄ ZAgCO (η^1-C)	−20.6	+0.6
7	ZAg + O_2 ⇄ $ZAgO_2$ (η^1-O)	−3.3	+10.8
8	ZAg + H_2O ⇄ $ZAgOH_2$ (η^1-O)	−17.4	−1.8
9	ZAg + N_2O ⇄ $ZAgN_2O$ (η^1-N)	−7.8	−0.9
10	ZAg + N_2O ⇄ $ZAgON_2$ (η^1-O)	−3.7	+0.1
11	$ZAgON_2$ (η^1-O) ⇄ ZAgO + N_2	−26.7	−9.7
12	ZAg + N_2O ⇄ ZAgO + N_2	+22.9	+9.8
13	ZAgON + NO ⇄ ZAgO + N_2O	+17.6	+35.8
14	ZAgON + NO ⇄ ZAgONNO	+10.9	+36.7
15	ZAgONNO ⇄ ZAgO + N_2O	+6.7	+0.2
16	ZAgNO + NO ⇄ ZAgO + N_2O	+26.1	+40.2
17	ZAgO + N_2O ⇄ $ZAgO_2$ + N_2	−59.1	−75.8
18	$ZAgO_2$ ⇄ ZAg + O_2	+3.3	−10.8
19	2NO ⇄ O_2 + N_2[a]	−42.1	−39.7

[a] At 298.15 K, the experimental Δ*H* and Δ*G* values for this reaction are −43.2 kcal/mol and −41.4 kcal/mol, respectively. The calculated values by us are Δ*H* = −42.3 kcal/mol and Δ*G* = −41.1 kcal/mol.

a crossing point of the singlet and triplet surfaces. This crossing point is related to the "transition state" and not to the initial and final reaction states. Therefore, it does not have any effect upon thermodynamic properties such as Δ*G* and Δ*H*.

N_2 elimination from $ZAgON_2$ (reaction 11) and ZAgO formation from ZAg + N_2O (reaction 12) are also spin forbidden since the fundamental state of ZAgO is a triplet whereas the fundamental states of $ZAgON_2$ as well as ZAg are both singlets. These reactions have been studied for Cu;[46,47] unfortunately, only energy changes were reported, and they cannot be compared with Δ*H* and Δ*G* values that include thermal corrections.

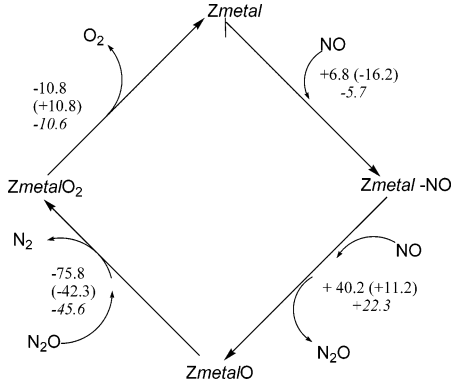

Figure 2. Bell−Chakraborty proposed pathway for NO decomposition. Numbers are Δ*G* values at 748 K in kcal/mol and Z(metal) = ZCu, ZAg, and ZAu. Plain numbers correspond to ZAg, Table 3. Numbers in parentheses correspond to ZCu, from ref 49. Italic numbers correspond to ZAu, Table 5.

Several mechanisms have been proposed for the NO decomposition over CuZSM-5. Schneider et al.[47,48] proposed that NO interacts with the ZCu to form the ZCuON species. This species react with another NO molecule to produces the ZCuONNO intermediate which subsequently decomposes into ZCuO + N_2O. According to the results presented in Table 3, this mechanism is unlikely for the AgZSM-5 catalyst. The formation of the ZAgON is not thermodynamically favored (Δ*G* = +11.1 kcal/mol) nor is the formation of the ZAgONNO intermediate (Δ*G* = +36.7 kcal/mol). Bell and Chakraborty[3,49] proposed a different pathway for NO_x decomposition over CuZSM-5. To test if the Bell−Chakraborty pathway applies for the AgZSM-5 catalyst, the same steps were considered. The corresponding Δ*H* and Δ*G* values are reported in Table 3 and shown in Figure 2. According to Bell and Chakraborty's results,[3,49] the first step in the catalytic cycle for CuZSM-5 is the NO adsorption. This adsorption is spontaneous with a $\Delta G_{ads} = -16.2$ kcal/mol. For

TABLE 4: Geometries, Atomic Charges, Vibrational Frequencies, and Spin Multiplicity (*S*) for the AuZSM-5 Model (ZAu)

molecular system	geometrical properties			Au charge	adsorbate charge	freq (cm^{-1})
ZAu	*R*(Au−Oa)	*R*(Au−Al) = 3.08 Å				
S = 1	2.28 Å	α(Oa-Au−Ob) = 70.4°		+0.77		
ZAuNO	*R*(Au−N)	*R*(N−O)	α(Au−N−O)	+0.85	−0.11	υ_{NO}
η^1-N, *S* = 2	1.98 Å	1.16 Å	134.1°			1855
ZAuON	*R*(Au−O)	*R*(N−O)	α(Au−O−N)			υ_{NO}
η^1-O, *S* = 2	2.23 Å	1.16 Å	132.6°	+0.78	−0.01	1829
$ZAu(NO)_2$	*R*(Au−N)	*R*(N−O)	α(Au−N−O)			υ_{NO}
η^1-N, *S* = 1	2.15 Å	1.15 Å	116.7°	+0.89	−0.07	1774
						1860
$ZAu(NO)_2$	*R*(Au−O)	*R*(N−O)	α(Au−O−N)			υ_{NO}
η^1-O, *S* = 1	2.37 Å	1.14 Å	129.1°	+0.73	+0.02	1764
						1889
ZAu(NO)(ON)	*R*(Au−O)	*R*(N−O)	α(Au−O−N)			υ_{NO}
η^1-O, *S* = 1	2.52 Å	1.13 Å	132.5°		+0.13	1775
				+0.76		
η^1-N	*R*(Au−N)	*R*(N−O)	α(Au−N−O)			
	2.06 Å	1.16 Å	120.2°		−0.13	1931
ZAuCO	*R*(Au−C)	*R*(C−O)	α(Au−C−O)			υ_{CO}
η^1-C, *S* = 1	1.90 Å	1.13 Å	179.9°	+0.77	+0.01	2188
$ZAuOH_2$	*R*(Au−O)	*R*(O−H)	α(Al−Au−O)	+0.62	+0.13	υ_{OH}
η^1-O, *S* = 1	2.15 Å	0.97 Å	143.1°			3788
$ZAuO_2$	*R*(Au−O)	*R*(O−O)	α(Au−O−O)	+0.82	−0.10	υ_{OO}
η^1-O, *S* = 3	2.13 Å	1.23 Å	123.5°			1444
$ZAuN_2O$	*R*(Au−N)	*R*(N−N)				υ_{NN}
η^1-N, *S* = 1	2.03 Å	1.12 Å	α(Au−N−N)	+0.72	+0.04	2302
		R(N−O)	173.3°			υ_{NO}
		1.17 Å				1317
$ZAuON_2$	*R*(Au−O)	*R*(N−N)	α(Au−O−N)	+0.68	+0.08	υ_{NN}
η^1-O, *S* = 1	2.23Å	1.12 Å	122.9°			2223
		R(N−O)				υ_{NO}
		1.20 Å				1213

AgZSM-5 this is not as favored as for CuZSM-5 (see Figure 2.) Consequently, the concentration of the metal−NO species must be lower for the AgZSM-5 than for the CuZSM-5 catalyst. In general, the lower activity of the AgZSM-5 catalyst compared to the CuZSM-5 catalyst is explained in terms of Ag^+ ion losses due to their transformation into silver particles.[28] The NO adsorption results show that the reduced activity could be an intrinsic limitation of the Ag catalyst instead. If NO adsorption is the first step in the catalytic cycle, the activity of the silver catalysts will be lower than the activity of the Cu catalyst since the metal-NO species concentration will always be lower for the AgZSM-5 than for the CuZSM-5 system. Only reactions 1, 16, 17, and 18 participate in the Bell−Chakraborty cycle. All these reactions are spin-allowed; that is, there are no spin changes, and consequently, the whole cycle is spin-allowed.

Gold(I) Zeolite. Table 4 shows some relevant geometrical properties, net charges and vibrational frequencies for the ZAu model. In general, the Au net charge is close to +1 and there occurs a charge transfers between the Au atom and the adsorbate. For example, the charge on Au increases from +0.77 e for ZAu to +0.85 e, +0.89 e, and +0.82 e for ZAuNO, $ZAu(NO)_2$, and $ZAuO_2$, respectively. In other cases, such as $ZAuOH_2$ and $ZAuON_2$, the Au atom is reduced. This change in the charge transfer from Au to the adsorbate or from the adsorbate to Au results from the propensity of Au(I) to be reduced as well as oxidized.

The calculated υ_{CO} value of 2188 cm^{-1} as well as the Au−C distance (1.90 Å) for ZAuCO are in reasonable agreement with published experimental values: 2178,[50] 2192,[20] 2190, 2176,[21] and 2170 cm^{-1} [22] and 1.92 and 1.93 Å.[51] Similarly, the calculated N−O frequencies of 1855 and 1829 cm^{-1} that correspond to ZAuNO and ZAuON are close to the experimental values of 1840, 1817,[22] and 1811 cm^{-1}.[23] For $ZAu(NO)_2$ η^1-N and $ZAu(NO)_2$ η^1-O, the symmetric and antisymmetric N−O stretching frequencies (1774 and 1860 cm^{-1} and 1764 and 1889 cm^{-1}) agree well with the experimental values of 1741 and 1837 cm^{-1}.[22] Noteworthy, unlike the $ZAu(NO)_2$ η^1-N and $ZAu(NO)_2$ η^1-O systems, the calculated value of 1931 cm^{-1} associated with the ZAu(NO)(ON) structure, is significantly higher than the experimental values of 1741 and 1837 cm^{-1}. Consequently, the reported experimental frequencies must correspond to an adsorption mode where both are η^1-N or both are η^1-O, but not to structures such as Au(NO)(ON).

Table 5 shows the thermodynamic values of ΔH and ΔG at 748 K for a selected set of reactions. According to these results, the adsorption of NO through the N atom is a spontaneous process ($\Delta G = -5.7$ kcal/mol) while the adsorption through the O atom is not thermodynamically favored ($\Delta G = +10.8$ kcal/mol) In general, the interactions of the adsorbent molecules with Au(I) are more exothermic than the corresponding interactions with Ag(I). Consequently, the processes tend to be more spontaneous for AuZSM-5 than for AgZSM-5. For example, the N_2O η^1-N adsorption on the ZAg model shows a free energy change of −0.9 kcal/mol (reaction 9, Table 3), while for the ZAu model, the ΔG value is −5.7 kcal/mol (reaction 27, Table 5). The interaction of ZAu with CO is a very favored process ($\Delta H = -45.3$ kcal/mol, $\Delta G = -21.5$ kcal/mol, reaction 25, Table 5), unlike the ZAg case, where ΔG is positive ($\Delta G = +0.6$ kcal/mol, reaction 6, Table 3). This is in agreement with the experimental fact that gold-supported catalysts promote CO oxidation while the silver catalysts are relatively inert toward this process.

The theoretical results for N_2O decomposition (reaction 30) indicate that this reaction proceeds at temperatures below 475°C (the estimated value of ΔG at 390 °C is −19 kcal/mol). This agrees with Schatler et al.'s results[21] who show that the N_2O can be decomposed by Au-MFI at temperatures below 396 °C.

Figure 2 displays the ΔG values associated with each of the steps in the Bell−Chakraborty proposed pathway for NO decomposition, for the CuZSM-5, AgZSM-5 and AuZSM-5

TABLE 5: Calculated ΔH and ΔG of Reaction (in kcal/mol) at 748 K for the AuZSM-5 Model (ZAu)

eq no.	reaction	ΔH (kcal/mol)	ΔG (kcal/mol)
20	ZAu + NO ⇄ ZAuNO (η^1-N)	−29.0	−5.7
21	ZAuNO (η^1-N) + NO ⇄ ZAu(NO)$_2$ (η^1-N)	−0.8	+25.2
22	ZAuNO (η^1-N) + NO ⇄ ZAu(NO)$_2$ (η^1-N;η^1-O)	+20.7	+41.6
23	ZAu + NO ⇄ ZAuON (η^1-O)	−8.1	+10.8
24	ZAuON (η^1-O) + NO ⇄ ZAu(ON)$_2$ (η^1-O)	+25.0	+46.4
25	ZAu + CO ⇄ ZAgCO (η^1-C)	−45.3	−21.5
25	ZAg + O_2 ⇄ ZAuO$_2$ (η^1-O)	−9.0	+10.6
26	ZAu + H_2O ⇄ ZAuOH$_2$ (η^1-O)	−28.8	−1.1
27	ZAu+ N_2O ⇄ ZAuN_2O (η^1-N)	−17.3	−5.7
28	ZAu+ N_2O ⇄ ZAuON_2 (η^1-O)	−7.8	+3.4
29	ZAuON_2 (η^1-O) ⇄ ZAuO + N_2	−1.0	−24.0
30	ZAu + N_2O ⇄ ZAuO + N_2	−8.8	−20.6
31	ZAuON + NO ⇄ ZAuO + N_2O	−10.0	+5.8
32	ZAuNO + NO ⇄ ZAuO + N_2O	+10.9	+22.3
33	ZAuO$_2$ ⇄ ZAu + O_2	+9.0	−10.6
34	ZAuO + N_2O ⇄ ZAuO$_2$ + N_2	−33.0	−45.6

catalytic systems. Values for the Cu catalyst were taken from ref 49, and serve as the reference.

For both, the ZAgO as well as the ZAuO model, the fundamental state is the triplet state; thus, similar considerations regarding spin-allowed and spin-forbidden reactions apply. Nevertheless, it is worthwhile to compare the behavior of the three metals in detail. The first step; that is, the NO adsorption, is thermodynamically favored for AuZSM-5, as it is in the Cu case. On the contrary, for the AgZSM-5 case, this step is not thermodynamically favored ($\Delta G = +6.8$ kcal/mol). The transformation of the Z(metal)−NO species into Z(metal)O through the addition of a second NO molecule is highly unfavorable for the AgZSM-5 model ($\Delta G = +40.2$ kcal/mol) and less unfavorable for Au and Cu. For the three metals, that is, Cu, Ag and Au, the reaction of the Z(metal)O species with N_2O to produce N_2 is thermodynamically spontaneous and follows the order $\Delta G_{Cu} > \Delta G_{Au} > \Delta G_{Ag}$. The last step, that is, the liberation of one O_2 molecule to produce the Z(metal) species, is an endothermic process in all three cases ($\Delta H > 0$) yet spontaneous for Ag and Au only.

It is well-known that water inhibits the decomposition of NO over CuZSM-5.[1,52,53] Theoretical studies performed on the CuZSM-5 catalyst[38] have revealed that the NO and the H_2O molecules compete for the active sites. Consequently, water deactivation results from a chemical equilibrium shift that favors H_2O adsorption. Calculation of the system's thermodynamic properties toward water adsorption allows the analysis of the H_2O interaction with the ZAg and ZAu catalysts. The results, shown below, demonstrate that the NO displacement reaction is a spontaneous processes for ZAgNO (reaction 35, $\Delta G = -8.6$ kcal/mol and $\Delta H = -4.9$ kcal/mol) but not for ZAuNO (reaction 36, $\Delta G = +4.6$ kcal/mol and $\Delta H = -0.2$ kcal/mol)

$$\text{ZAgNO} + \text{H}_2\text{O} \rightarrow \text{ZAgOH}_2 + \text{NO} \quad (35)$$

$$\text{ZAuNO} + \text{H}_2\text{O} \rightarrow \text{ZAuOH}_2 + \text{NO} \quad (36)$$

The calculated equilibrium constants for reactions 35 and 36 are $K_{eq}(\text{Ag}) = 3.25 \times 10^2$, $K_{eq}(\text{Au}) = 4.5 \times 10^{-2}$, respectively. This reveals that water displaces the adsorbed NO more easily from ZAgNO than from ZAuNO; thus, deactivating the silver catalyst more readily than the gold catalyst.

Conclusions

Main geometric parameters, thermodynamic properties and vibrational frequencies were determined for the Ag^IZSM-5 and Au^IZSM-5 models and their interactions with CO, NO, O_2, N_2O, and H_2O molecules, using DFT. The calculated vibrational frequencies agree with the experimental values, which validates the model used; that is, the model mimics with certain degree of confidence the actual catalytically active site.

The calculated results show that both, NO and N_2O interact more favorably with Au(I) than with Ag(I.) Moreover, NO adsorption is thermodynamically less favored on Ag^IZSM-5 than on the Cu^IZSM-5, whereas the adsorption on Au(I) and on Cu^I-ZSM-5 are comparable.

Additionally, the theoretical calculations reveal that N_2O decomposition into N_2 is feasible at temperatures below 475 °C for the Au^IZSM-5 but not for the Ag^IZSM-5 catalyst. Accordingly, the Au catalyst should perform similarly to the Cu catalyst for NO_x reduction. Results also show that H_2O molecules displace the adsorbed NO less easily from Au than from Ag; thus, the Au catalyst should be more resistant toward water deactivation than the Ag catalyst.

The practical limitation for the use of the Au catalyst resides in Au(I)'s susceptibility toward reduction to Au(0). This limitation could be potentially overcome using excess O_2 in the reaction[23] or through the addition of certain promoters that stabilize the oxidized metal state, such as Ce in the case of the AgZSM-5 catalyst.[28] As Shelef[1] states: "The aim, common to all heterogeneous catalysts, is to stabilize the catalytically active centers without impairing the activity".

Acknowledgment. The authors acknowledge the financial support given by Proyecto Alma Mater and FONACIT Proyecto G-2005000426.

References and Notes

(1) Shelef, M. *Chem. Rev.* **1995**, *95*, 209.
(2) Parvulescu, V. I.; Grange, P.; Delmon, B. *Catal. Today* **1998**, *46*, 233.
(3) Bell, A. T. *Catal. Today* **1997**, *38*, 151.
(4) Zhu, Z.; Liu, Z.; Niu, H.; Liu, S.; Hu, T.; Liu, T.; Xie, Y. *J. Catal.* **2001**, *197*, 6.
(5) Maunula, T.; Ahola, J.; Hamada, H. *Appl. Catal., B* **2000**, *26*, 173.
(6) Gómez, S. A.; Campero, A.; Martínez-Hernández, A.; Fuentes, G. A. *Appl. Catal., A* **2000**, *197*, 157.
(7) Yahiro, H.; Iwamoto, M. *Appl. Catal., A* **2001**, *222*, 163.
(8) Shelef, M. *Catal. Lett.* **1992**, *15*, 305.
(9) Lombardo, E.; Sill, G.; D'Itri, J.; Hall, W. K. *J. Catal.* **1998**, *173*, 440.
(10) Feng, X.; Hall, W. K. *J. Catal.* **1997**, *166*, 368.
(11) Joyner, R. W.; Stockernhuber, M. *Catal. Lett.* **1997**, *45*, 15.
(12) Hall, W. K.; Feng, X.; Dumesic, J.; Watwe, R. *Catal. Lett.* **1998**, *52*, 13.
(13) Volodin, A. M.; Sobolev, V. I.; Zhidomirov, G. M. *Kinet. Catal.* **1998**, *39*, 775.
(14) Chen, H. Y.; El-Malki, El-M.; Wang, X.; van Santen, R. A.; Sachtler, W. M. H. *J. Mol. Catal. A* **2000**, *162*, 159.

(15) Lukyanov, D.; Lombardo, E.; Sill, G.; D'Itri, J.; Hall, W. K. *J. Catal.* **1996**, *163*, 447.
(16) Lombardo, E.; Sill, G.; D'Itri, J.; Hall, W. K. *J. Catal.* **1998**, *173*, 440.
(17) Li, Y.; Armor, J. N. *Appl. Catal., B* **1993**, *2*, 239.
(18) Li, Y.; Armor, J. N. *Appl. Catal., B* **1992**, *1*, L31.
(19) Li, Y.; Salger, T. L.; Armor, J. N. *J. Catal.* **1994**, *150*, 388.
(20) Mohamed, M. M.; Salama, T. M.; Ichikawa, M. *J. Colloid Interface Sci.* **2000**, *224*, 366.
(21) Gao, Z.-X.; Sun, Q.; Chen, H.-Y.; Wang, X.; H Sachtler, W. M. *Catal. Lett.* **2001**, *72*, 1.
(22) Qiu, S.; Ohnishi, R.; Ichikawa, M. *J. Phys. Chem. Lett.* **1994**, *98*, 2719.
(23) Salama, T. M.; Ohnishi, R.; Ichikawa, M. *Chem. Commun.* **1997**, 105.
(24) Salama, T. M.; Ohnishi, R.; Shido, T.; Ichikawa, M. *J. Catal.* **1996**, *162*, 169.
(25) Shi, C.; Cheng, M.; Qu, Z.; Bao, X. *Appl. Catal., B* **2004**, *51*, 171.
(26) Furusawa, T.; Seshan, K.; Lercher, J. A.; Lefferts, L.; Aika, K. *Appl. Catal., B* **2002**, *37*, 205.
(27) Furusawa, T.; Lefferts, L.; Seshan, K.; Aika, K. *Appl. Catal., B* **2003**, *42*, 25.
(28) Li, Z.; Flytzani- Stephanopoulos, M. *J. Catal.* **1999**, *182*, 313.
(29) Shi, C.; Cheng, M.; Qu, Z.; Bao, X. *J. Mol. Catal.* **2005**, *235*, 35.
(30) Matsuoka, M.; W−S. Ju, Yamashita, H.; Anpo, M. *J. Photochem. Photobiol. A Chemistry* **2003**, *160*, 43.
(31) Shibata, J.; Takada, Y.; Shichi, A.; Satokawa, S.; Satsuma, A.; Hattori, T. *J. Catal.* **2004**, *222*, 368.
(32) Shibata, J.; Shimizu, K.; Takada, Y.; Shichi, A.; Yoshida, H.; Satokawa, S.; Satokawa, S.; Satsuma, A.; Hattori, T. *J. Catal.* **2004**, *227*, 367.
(33) Zhanpeisov, N. U.; Martra, G.; Ju, W. S.; Matsuoka, M.; Coluccia, S.; Anpo, M. *J. Mol. Catal. A* **2003**, **201**, 237.
(34) W−S. Ju, Matsuoka, M.; Iiono, K.; Yamashita, H.; Anpo, M. *J. Phys. Chem. B* **2004**, *108*, 2128.
(35) Matsuoka, M.; Ju, W.-S.; Anpo, M. *Chem. Lett.* **2000**, 626.
(36) Kanan, S. M.; Omary, M. A.; Patterson, H. H.; Matsuoka, M.; Anpo, M. *J. Phys. Chem. B* **2000**, *104*, 3507.
(37) Gaussian 98, Revision A.11.4, Frisch, M. J.; Trucks, G. W.; Schlegel, H. B.; Scuseria, G. E.; Robb, M. A.; Cheeseman, J. R.; Zakrzewski, V. G.; Montgomery, J. A., Jr.; Stratmann, R. E.; Burant, J. C.; Dapprich, S.; Millam, J. M.; Daniels, A. D.; Kudin, K. N.; Strain, M. C.; Farkas, O.; Tomasi, J.; Barone, V.; Cossi, M.; Cammi, R.; Mennucci, B.; Pomelli, C.; Adamo, C.; Clifford, S.; Ochterski, J.; Petersson, G. A.; Ayala, P. Y.; Cui, Q.; Morokuma, K.; Rega, N.; Salvador, P.; Dannenberg, J. J.; Malick, D. K.; Rabuck, A. D.; Raghavachari, K.; Foresman, J. B.; Cioslowski, J.; Ortiz, J. V.; Baboul, A. G.; Stefanov, B. B.; Liu, G.; Liashenko, A.; Piskorz, P.; Komaromi, I.; Gomperts, R.; Martin, R. L.; Fox, D. J.; Keith, T.; Al-Laham, M. A.; Peng, C. Y.; Nanayakkara, A.; Challacombe, M.; Gill, P. M. W.; Johnson, B.; Chen, W.; Wong, M. W.; Andres, J. L.; Gonzalez, C.; Head-Gordon, M.; Replogle, E. S.; Pople, J. A. Gaussian, Inc.: Pittsburgh, PA, 2002.
(38) Sierraalta, A.; Bermudez, A.; Rosa-Brussin, M. *J. Mol. Catal. A* **2005**, *228*, 203.
(39) Sierraalta, A.; Añez, R.; Rosa-Brussin, M. *J. Catal.* **2002**, *205*, 107.
(40) Sierraalta, A.; Añez, R.; Rosa-Brussin, M. *J. Phys. Chem. A* **2002**, *106*, 6851.
(41) Solans-Monfort, X.; Branchadell, V.; Sodupe, M. *J. Phys. Chem. B* **2002**, *106*, 1372.
(42) Solans-Monfort, X.; Branchadell, V.; Sodupe, M. *J. Phys. Chem. A* **2000**, *104*, 3225.
(43) Nachtigall, P.; Nachtigallová, D.; Sauer, J. *J. Phys. Chem. B* **2000**, *104*, 1738.
(44) Bolis, V.; A Barbaglia., Bordiga, S.; Lamberti, C.; Zecchina, A. *J. Phys. Chem. B* **2004**, *108*, 9970.
(45) Akolekar, D. B.; Bhargava, S. K. *J. Mol. Catal. A* **2000**, *157*, 199.
(46) Solans-Monfort, X.; Sodupe, M.; Branchadell, V. *Chem. Phys. Lett.* **2003**, *368*, 242.
(47) Schneider, W. F.; Hass, K. C.; Ramprasad, R.; Adams, J. B. *J. Phys. Chem. B* **1998**, *102*, 3692.
(48) Schneider, W. F.; Hass, K. C.; Ramprasad, R.; Adams, J. B. *J. Phys. Chem. B* **1997**, *101*, 4353.
(49) Trout, B. L.; Chakraborty, A. K.; Bell, A. T. *J. Phys. Chem.* **1996**, *100*, 17582.
(50) Fierro-Gonzalez, J. C.; B. Andersonb, G.; Rameshb, K.; Vinodb, C. P.; Niemantsverdrietb, J. W.; Gates, B. C. *Catal. Lett.* **2005**, *101*, 265.
(51) Fierro-Gonzalez, J. C.; Gates, B. C. *J. Phys. Chem. B Lett.* **2004**, *108*, 16999.
(52) Gómez, S. A.; Campero, A.; Martínez-Hernández, A.; Fuentes, G. A. *Appl. Catal., A* **2000**, *197*, 157.
(53) Subbiah, A.; Cho, B. K.; Blint, J. R.; Gujar, A.; Price, G.; Yie, J. E. *Appl. Catal., B* **2003**, *42*, 155.
(54) Satsuma, A.; Shibata, J.; Shimizu, K.-i; Hattori, T. *Catal. Survey Asia* **2005**, 75.
(55) Citra, A.; Andrews, L. *J. Phys. Chem. A* **2001**, *105*, 3042.
(56) Citra, A.; Wang, X.; Andrews, L. *J. Phys. Chem. A* **2002**, *106*, 3287.
(57) Liang, B.; Andrews, L. *J. Phys. Chem. A* **2000**, *104*, 9156.
(58) NIST Computational Chemistry Comparison and Benchmark Database, NIST Standard Reference Database Number 101, Release 12, Aug 2005, Johnson, R. D., III, Ed.; http://srdata.nist.gov/cccbdb.